USE OF NANO-ANATASE IN DEGRADATION OF HETEROCYCLIC DYES FROM WATERS

Claudia Ionela TARCEA[1], Cristian PREDESCU[1], Ecaterina MATEI[1], Andra Mihaela PREDESCU[1], Maria RAPA[1], Andreea TURCANU[1]

The presence of heterocyclic dyes as refractory pollutants into wastewaters represent a serious problem of the biodegradability of the waters. The photocatalytic activity and chemistry surface of nano-anatase as photoacatalyst become more and more attractive option for degradation process. Thus, the steps of the synthesis, characterization and applications are necessary being investigated in detail. The production of a single–controlled phase as anatase was synthesized due its strong photocatalytic properties. The morphology, size and elemental composition were monitored by scanning electron microscopy [SEM] and Energy dispersive X-ray spectroscopy [EDS]. In order to identify the crystal structure, X-ray diffraction [XRD] was used and Zeta potential measurements were used for estimating agglomeration tendency and surface stability. The photocatalytic activity of nano-anatase was evaluated by measuring the degradation tendency of methylene blue. Good results were achieved regarding the degradation efficiency.

Keywords: nano-anatase, heterocyclic dye, photocatalytic activity

1. Introduction

Heterocyclic dyes are a group of organic pollutants which are present in the textile, paper and cosmetic industries being useful to give color of the products. In the last years a great attention has been focused on their presence as main pollutant in above-mentioned industries due to potential toxicity induced by concentrations and color intensity. The textile industry generates an exponential increase of colored wastewater and the effluents of products affects entire ecosystem [1]. An important research goal is finding an effective treatment method.

A more effectiveness and promising technique than classical processes to removal color from textile effluents is represented by advanced oxidation processes (AOPs) [2-3]. The main advantage of AOP is achieving one of the important concept regarding „zero pollution" [4] by avoiding the transfer of pollutant from one phase to another, based on producing of hydroxyl radicals that oxidizes the organic pollutant in short time [5-6]. Mainly, the AOP process consist of use a metal oxide semiconductors with high ability to generate holes and

[1] Faculty of Material Science and Engineering, University POLITEHNICA of Bucharest, Romania, e-mail: tarceaclaudia@yahoo.com

electrons under photocatalytic conditions. Subsequently to the process, water and oxygen molecules are decomposed by forming species such as, OH•, H_2O_2 and $O_2^{\cdot -}$ on the surface of the catalyst. In the end these species have the power to completely decomposed/mineralized organic pollutants. Among the many semiconductors (CeO_2, ZnO, CdS, Fe_3O_4), TiO_2 is considered to be the most attractive catalyst because of its low-cost, strong photocatalytic activity and stability [7-11].

Methylene blue (MB) represents colorant widely spread in wastewaters with a heterocyclic structures from cationic thiazine group which could be degraded in a simple structures as single cycle rings under UV conditions.

This research was focused on the synthesis, characterization and testing of a single-phase anatase as nanostructured photocatalyst. The photocatalytic activity was studied by degradation of methylene blue as heterocyclic dye under UV irradiation.

2. Experiment

2.1. Materials and methods

In this research all chemicals were of analytical grade and used without further purification. Methylene Blue (M. wt of 319.86; molecular formula of $C_{16}H_{18}ClN_3S•xH_2O$; λmax of 663–667 nm; cationic) was purchased by Merck. TiO_2 as Nano-anatase was prepared using sol-gel method according with [12]. Briefly, 5 mL of Titanium tetra iso-propoxide [$Ti(OCH(CH_3)_2]_4$, Sigma-Aldrich, 97%] was added into a mixture of acetic acid (5 mL) [CH_3COOH, Sigma-Aldrich] and ethanol (50 mL) [C_2H_5OH, Sigma- Aldrich] after the mixture was continuous stirred for 30 min; dilute ammonia aqueous solution [NH_3, Sigma-Aldrich] 1N was then added to achieve the pH 10. The precipitate was washed thoroughly with distilled water and ethanol before dried at 100˚C. The powder was calcined at 550˚C for 1h to improve the crystallinity of the nano-anatase using an oven MICROTERM 1206 with maximum temperature 1000˚C.

The distribution, morphology, purity and size of particles of nano-anatase have been characterized using SEM (scanning electron microscopy), XRD (X-ray diffraction). Photocatalytic degradation of MB was investigated by Ultraviolet-Visible spectrometry and kinetic study.

The structural characterization of the nano-anatase was performed by the X-ray diffraction (PANalytical X'Pert PRO) using the following conditions: Cu K_α radiation (λ = 1.5418 Å), the voltage 45 kV and the current were kept at 40 Ma from 20-90˚C. The average crystallite size was calculated according to the Debye–Scherrer's Eq. (1)

$$D = K\lambda / (\beta \cos\theta) \quad (1)$$

where K is the Scherrer's constant, λ the X-ray wavelength, β is the peak width at half-maximum and θ is the Bragg diffraction angle.

Scanning electron microscope (SEM) analysis was acquired using a FEI Quanta FEG 450 microscope for determining the morphological and size of the surface nano-anatase.

The surface change of the nano-anatase was examined using Zetasizer Nano series (Zetasizer Nano, Malvern Instruments, UK). The pH was adjusted using solutions of NaOH and H_2SO_4.

The photocatalytic activity of nano-anatase was investigated varying the parameters which influence the photocatalytic degradation of methylene blue solution such as dosage of catalyst, concentrations of dye and contact time of irradiation. All the experiments were conducted in 50 ml solution under air bubbled for 30 min in dark condition to obtain the adsorption-desorption equilibrium and then was irradiated under UV lamp (75W, Philips) with visible light source (λ = 365 nm), during 60 min. Every 15 minute the sample were taken, separated and measured identifying the UV-VIS spectrum peaks.

The photocatalytic activity of the nano-anatase was evaluated by monitoring the degradation of MB using UV-VIS spectrophotometer at 665 nm. The photocatalytic degradation of MB was calculated by Eq. 2:

$$\% \ MB \ Efficiency = \frac{C_0 - C_t}{C_0} x100 \quad (2)$$

where C_0 is he initial MB concentration (mg/L), C_t is MB concentration at various time t (min).

Kinetic study in photocatalytic degradation of MB helps to investigate the parameters such as the reaction rate constant k (min^{-1}) and regression coefficient R^2. The pseudo-first order kinetic was proposed by [13] Eq. 3

$$ln\frac{C_t}{C_0} = -k_1 t \quad (3)$$

Pseudo-first-order plot of ln C_t/C_0 versus t was given a linearity from which k_1 (min^{-1}) can be calculated from the slope.

3. Results and discussion

3.1. X-ray diffraction XRD

The composition and the phase structural of nano-anatase were investigated using XRD patterns as it was given in Fig. 1. The pattern indicates a single–controlled phase with distinctive peaks located at 2θ – 25.35, 38.64, 48.14, 53.97 and 55.18 which was attributed to anatase phase (101), (112), (200), (105) and (204) according to the peak list ICSD 76173. From, the Debye-Scherer's formula, the average crystallite sizes observed around 9 nm.

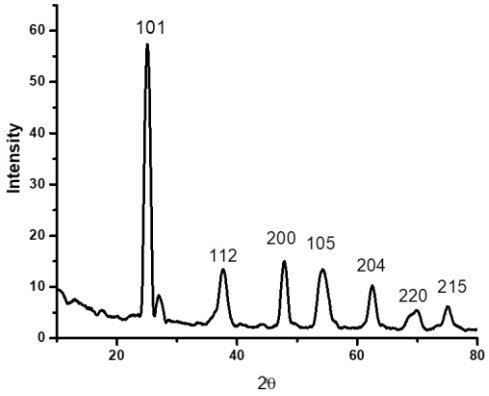

Fig. 1. XRD patterns of nano-anatase

3.2. Zeta potential

To elucidate the charge processes and interactions between the solid/lichid were used Zeta potential analysis. Fig. 2 presented the pH at which the zeta potential of nano-anatase shifted to zero (pHpzc).

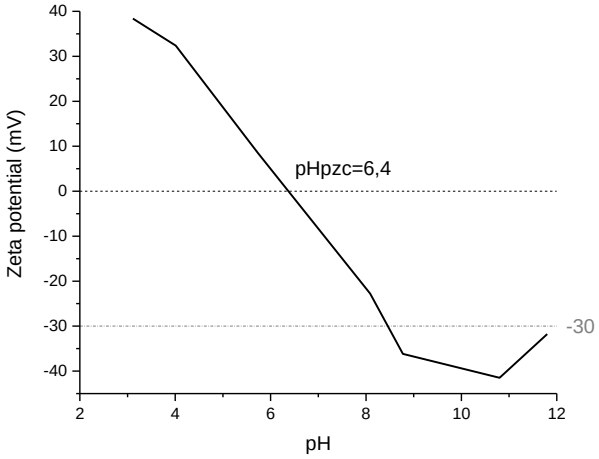

Fig. 2. Zeta potential of nano-anatase versus pH

According to the literature [14] stability of colloids and nanoparticles appears when zeta potential is typically more than 30 mV. In our case the nanoparticles of nano-anatase exposed stability between 32.36 - 38.4 mV and (-31.76) – (-41.5) of Zeta potential which indicated that the nanoparticles are not dissolved under acidic conditions (pH 4 – 3.1) and under strong basic conditions

(pH 10.8-11.8). Also, the pHpzc with 6.4 value indicates that our material is protonated strongly under acidic conditions (below 6.4) in comparison with hydroxylated surface (above 6.4), where the surface is compatible for attraction of methylene blue protonated groups. This is validated by the surface analysis of the material, as it is indicated in pointed line. The zeta potential analysis exhibited the transition the positive potential at low pH to the negative potential at high pH. The zeta potential analysis exhibited the transition the positive potential at low pH to the negative potential at high pH.

3.3. Scanning electron microscopy (SEM)

Fig. 3 (a), (b) shows SEM imagines of the surface of nano-anatase initial and after contact with MB. Initial nano-anatase shown a similar and uniform surface while after contact with MB it shows a tendency of agglomeration Fig. 3 b. The size of the formed nano-anatase was within the range of 10-40 nm.

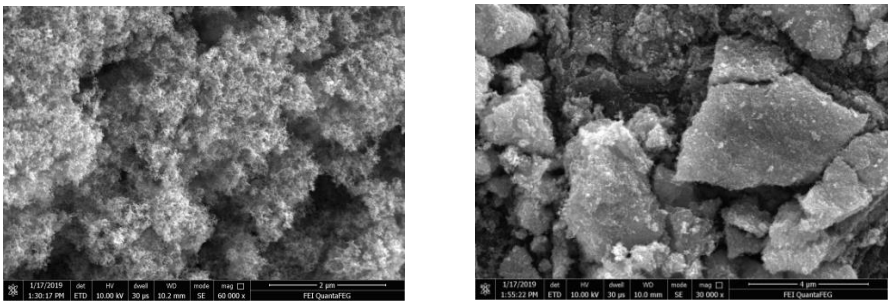

Fig. 3. SEM images of nano-anatase (a) before and (b) after contact time with MB

3.4. Photocatalytic activity of nano-anatase

Effect of different concentration of MB

The photocatalytic activity of nano-anatase was measured based on the reaction rate of the photocatalytic degradation of MB. It is clearly observed that the MB efficiency increases with irradiation time, demonstrating the photocatalytic degradation of MB. Fig. 4, shows that MB efficiency was reduced from 99.72 to 78% with increasing the concentrations from 0.5 to 8 mg/L after 60 min.

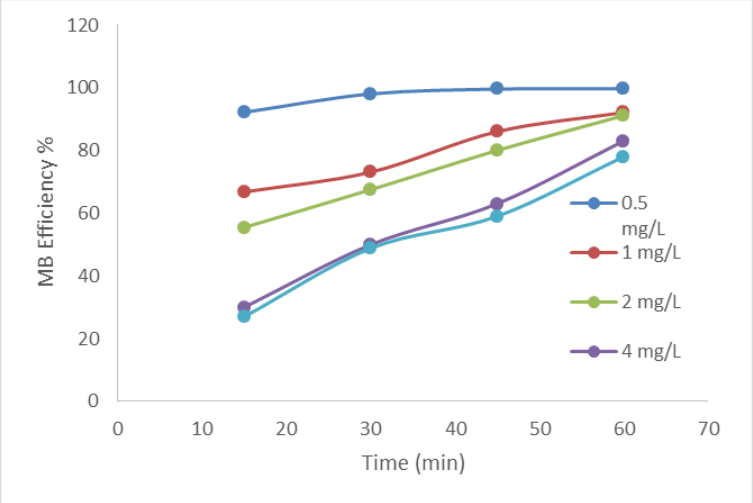

Fig. 4. Dye MB efficiency at different initial concentration

From the plot of the –ln(C/C0) against irradiation time up to 60 min was demonstrated that increasing the MB concentrations resulted a linearity decreased rate constant Fig. 5. Similar trends has been reported by [15-16].

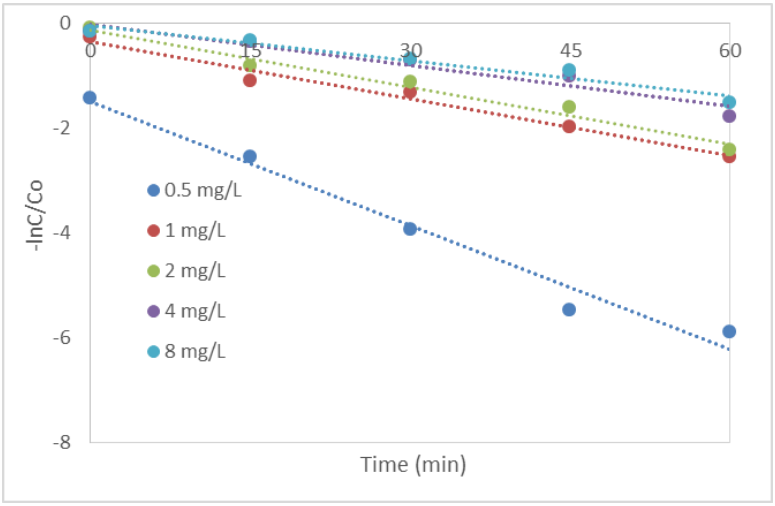

Fig. 5. Plots of pseudo-first order kinetics at different initial MB concentrations

The rate constants and the corresponding correlation coefficients (R^2) were calculated from the plots and are listed in Table 1. From the results obtained, the pseudo-first-order kinetic was fitted well for concentrations between 0.5-2 mg/L.

Table 1

The values of first-pseudo order constants and the corresponding correlation coefficients for the photocatalytic degradation of MB

C (mg/L)	k_1 (min $^{-1}$)	R^2
0.5	0.0789	0.976
1	0.0361	0.977
2	0.0364	0.978
4	0.0260	0.936
8	0.0221	0.950

The effect of nano-anatase dosage

Fig. 6 shows the photocatalytic degradation of 2 mg/L MB during 60 min irradiation time, according to kinetic results. It is obviously that the photocatalytic degradation depends on the surface area of nano-anatase due to a large nano-anatse dosage produce more hydroxyl radical and electrons which absorb more photons [17].

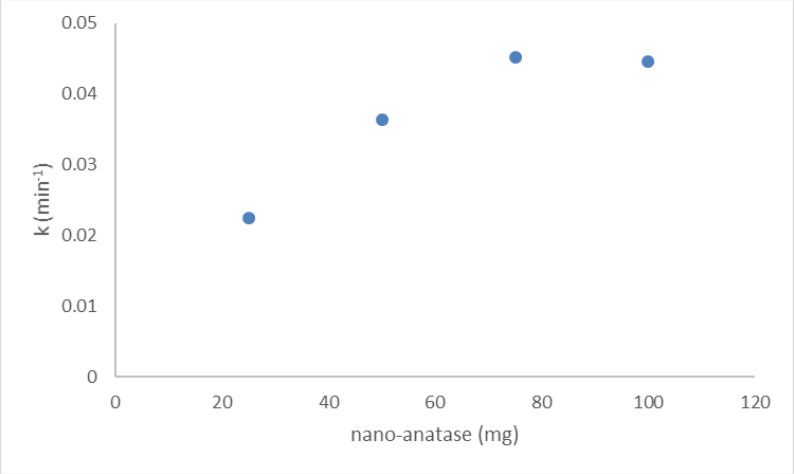

Fig. 6. Plot of k as a function TiO_2 dosage

However, it should be mentioned that an excessive nano-anatase dosage can decrease the degradation due to turbidity of solution and it is necessary higher light power or larger number of photons for exciting the nano-anatase. The tendency could be observed in Fig. 5 where k values increased up to 75 mg and then the rate constant will be saturated and decreased at larger nano-anatase dosage [18].

3.5. Photocatalytic stability of nano-anatase

To confirm the photocatalytic stability of the nano-anatase the experiments were performed under irradiation conditions and maintained after three cycles of photocatalytic degradation of MB.

From Fig. 7 it can be observed that the photocatalytic degradation of MB by nano-anatase depends on the contact time. In the first cycle with increasing time, the photocatalytic degradation of MB increases from 43 to 89% and drops below 39% in the third cycle after 60 minutes.

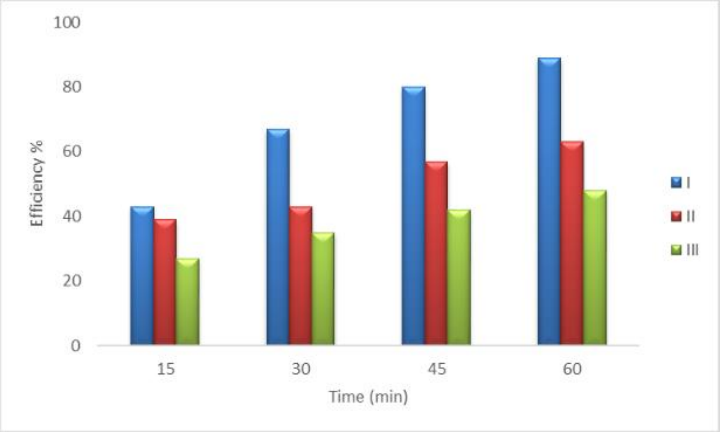

Fig.78. Efficiency (%) of nano-anatase for MB degradation cycles

4. Conclusion

The aim of this research was to synthesis single–controlled phase as anatase as photocatalyst. The morphology, structural, charge surface, size and purity of nano-anatase and the characteristic peaks of MB have been characterized using XRD (X-ray diffraction), SEM (Scanning electron microscopy), Zeta Potential and UV-VIS spectrometry. SEM analysis indicated an agglomeration of nanoparticles with size 10-40 nm, these values being correlated with XRD analysis which indicated anatase as single phase with crystallite size about 9 nm. As anticipated, photocatalytic activity of nano-anatase shows a high photocatalytic activity in degradation MB. The results show that the maximum efficiency (99.72%) was found at low concentration of methylene blue (0.5 mg/L) after irradiation time as 60 min with amount of nano-anatase of 25 mg. The results show that the photocatalytic degradation of MB is determined by the ratio between the initial MB concentration and nano-anatase dosage

Acknowledgment

This work was supported by a grant of the Romanian Ministry of Research and Innovation, CCCDI-UEFISCDI, project number 26PCCDI/01.03.2018, "Integrated and sustainable processes for environmental clean-up, wastewater reuse and waste valorization" (SUSTENVPRO), within PNCDI III

R E F E R E N C E S

[1]. *M. A. Chia and R. I. Musa*, Effect of indigo dye effluent on the growth, biomass production and phenotypic plasticity of scenedesmus quadricauda (chlorococcales). Anais da Academia Brasileira de Ciências, ***86.*** (1), 2014**,** pp. 419-428.

[2]. C. Covaliu; I. Moga; M. Matache; G. Paraschiv; I. Gageanu and E. Vasile In *Synthesis and technological innovation of applying oxide nanomaterials in wastewater treatment by flotation*, IOP Conference Series: Materials Science and Engineering, IOP Publishing: 2018; p 012062.

[3]. *F. Ilie and C. Covaliu*, Tribological properties of the lubricant containing titanium dioxide nanoparticles as an additive. Lubricants, ***4.*** (2), 2016**,** pp. 12.

[4]. *J. E. Cobb and R. L. Byberg*, Photocatalytic degradation of a series of direct azo dyes using immobilized tio2. 2012**,** pp.

[5]. *A. Akyol*, Treatment of paint manufacturing wastewater by electrocoagulation. Desalination, ***285.*** 2012**,** pp. 91-99.

[6]. *W. Kuo and P. Ho*, Solar photocatalytic decolorization of methylene blue in water. Chemosphere, ***45.*** (1), 2001**,** pp. 77-83.

[7]. *J.-M. Herrmann*, Heterogeneous photocatalysis: State of the art and present applications in honor of pr. Rl burwell jr.(1912–2003), former head of ipatieff laboratories, northwestern university, evanston (ill). Topics in catalysis, ***34.*** (1-4), 2005**,** pp. 49-65.

[8]. *S.-i. Naya; A. Inoue and H. Tada*, Self-assembled heterosupramolecular visible light photocatalyst consisting of gold nanoparticle-loaded titanium (iv) dioxide and surfactant. Journal of the American Chemical Society, ***132.*** (18), 2010**,** pp. 6292-6293.

[9]. *D. Yang; H. Liu; Z. Zheng; Y. Yuan; J.-c. Zhao; E. R. Waclawik; X. Ke and H. Zhu*, An efficient photocatalyst structure: Tio2 (b) nanofibers with a shell of anatase nanocrystals. Journal of the American Chemical Society, ***131.*** (49), 2009**,** pp. 17885-17893.

[10]. *X. Han; Q. Kuang; M. Jin; Z. Xie and L. Zheng*, Synthesis of titania nanosheets with a high percentage of exposed (001) facets and related photocatalytic properties. Journal of the American Chemical Society, ***131.*** (9), 2009**,** pp. 3152-3153.

[11]. *W. Li; Y. Deng; Z. Wu; X. Qian; J. Yang; Y. Wang; D. Gu; F. Zhang; B. Tu and D. Zhao*, Hydrothermal etching assisted crystallization: A facile route to functional yolk-shell titanate microspheres with ultrathin nanosheets-assembled double shells. Journal of the American Chemical Society, ***133.*** (40), 2011**,** pp. 15830-15833.

[12]. *S.-H. Lee; C. Tekmen and W. M. Sigmund*, Three-point bending of electrospun tio2 nanofibers. Materials Science and Engineering: A, ***398.*** (1-2), 2005**,** pp. 77-81.

[13]. *J. Singh; Y.-Y. Chang; J. R. Koduru and J.-K. Yang*, Potential degradation of methylene blue (mb) by nano-metallic particles: A kinetic study and possible mechanism of mb degradation. Environmental Engineering Research, ***23.*** (1), 2017**,** pp. 1-9.

[14]. A. Prokop; E. Kozlov; G. Carlesso and J. M. Davidson, Hydrogel-based colloidal polymeric system for protein and drug delivery: Physical and chemical characterization,

permeability control and applications. In *Filled elastomers drug delivery systems*, Springer: 2002; pp 119-173.

[15]. *R. Dariani; A. Esmaeili; A. Mortezaali and S. Dehghanpour*, Photocatalytic reaction and degradation of methylene blue on tio2 nano-sized particles. Optik, ***127.*** (18), 2016**,** pp. 7143-7154.

[16]. *K. Dai; L. Lu and G. Dawson*, Development of uv-led/tio 2 device and their application for photocatalytic degradation of methylene blue. Journal of materials engineering and performance, ***22.*** (4), 2013**,** pp. 1035-1040.

[17]. *T.-C. An; X.-H. Zhu and Y. Xiong*, Feasibility study of photoelectrochemical degradation of methylene blue with three-dimensional electrode-photocatalytic reactor. Chemosphere, ***46.*** (6), 2002**,** pp. 897-903.

[18]. *S. Parra; J. Olivero and C. Pulgarin*, Relationships between physicochemical properties and photoreactivity of four biorecalcitrant phenylurea herbicides in aqueous tio2 suspension. Applied Catalysis B: Environmental, ***36.*** (1), 2002**,** pp. 75-85.